

Fabrication of three-dimensional WO₃ nanotube bundles on carbon cloth as binder-free electrode for high-performance supercapacitor

Jin Li,^{*a} Jie Luo^{‡b} and Shuo Yan^a

^aCollege of Chemistry and Chemical Engineering, and Henan Key Laboratory of Function-Oriented Porous Materials, Luoyang Normal University, Luoyang 471934, China

^bSchool of Chemical Engineering and Pharmaceutics, Henan University of Science and Technology, Luoyang 471023, China

[‡]These authors contributed equally to this work

*Corresponding author

Experimental Section

All chemicals were analytical grade and were used as received without further purification. Prior to the synthesis, a piece of carbon cloth with a size of 5 cm × 4 cm was cleaned with a 3 M HCl solution, ethanol and deionized water for 30 minutes, respectively. Typically, Na₂WO₄ (0.34 g) and NaHSO₃ (0.2 g) were dissolved in the mixture solution of deionized water (30 mL) and H₂O₂ (5 mL) under vigorous magnetic stirring. The above solution and the pretreated carbon cloth were then transferred into a 50 mL Teflon lined stainless autoclave and maintained at 180 °C for 24 h. After cooling to room temperature, the carbon cloth coated with WO₃ was taken out and washed with ethanol and deionized water several times, and dried. The loading weight on the carbon cloth was about 2.8 mg cm⁻². Furthermore, the WO₃ powders also were synthesized without carbon cloth at the same experimental condition.

Materials Characterizations

The energy dispersive X-ray (EDX) mapping and morphologies were investigated by field emission scanning electron microscopy (FESEM, ZEISS-Merlin) and transmission electron microscopy (TEM, JEOL, JEM-2100F). X-ray diffraction (XRD) measurements were characterized on a Bruker D8 advance setup. X-ray photoelectron spectroscopy (XPS) measurements were tested on a Perkin-Elmer Model PHI 5600 XPS system with a resolution of 0.3–0.5 eV from a monochromatic aluminum anode X-ray source. Raman spectroscopy (Jobin Yvon, T64000 spectrometer with a 514.5 nm argon ion laser) was used to characterize the products.

Electrochemical Measurement

Electrochemical measurements were carried out in a standard three-electrode system with an electrochemical workstation CHI 660e in 0.5 M H₂SO₄ solution at room temperature. A saturated calomel electrode (SCE), graphite rod, and the as-prepared samples were served as reference electrode, counter electrode, and working electrode, respectively. The cyclic voltammetry (CV) curves were conducted between 0.1 and -0.7 V. The galvanostatic charge-discharge (GCD) curves were measured at different current densities (0.5–10 A g⁻¹). Electrochemical impedance spectroscopy (EIS) was carried out at open circuit potential in the frequencies from 0.01 Hz to 100 kHz and the amplitude of the potential perturbation was 5 mV. The specific capacitance (C_{sp}) of electrodes was calculated from charge–discharge curves using the following equation: C_{sp} = (I × Δt)/(m × ΔV), where I is the discharge current, m is the mass of the electroactive material in the electrode, ΔV is the potential window, and Δt is the discharge time. During the galvanostatic charge/discharge of supercapacitors, the energy density (E) and power density (P) were calculated by the following equations: E = C_{sp} × ΔV²/7.2 (Wh Kg⁻¹), P = E × 3600/Δt (W Kg⁻¹). For comparison, 80 mg of WO₃ nanotube bundles was weighed by an electronic balance. Subsequently, the active material, polyvinylidene fluoride, and carbon black (8:1:1 weight ratio) were mixed in isopropyl alcohol to form homogeneous slurry. Then the slurry was painted onto CC (denoted as WNB). Finally, the electrode was dried in air at 80 °C for 12 h. Electrode area was 1.0 cm², and the mass of active material was about 2.8 mg.

Two pieces of WO₃ nanotube bundles electrode (area of 0.64 cm²) were put into a button cell, with a separator between them (NKK, TF4840) and 0.5 M H₂SO₄ aqueous solution as the electrolyte. After that, the unsealed button cell was transferred to a hydraulic crimping machine and sustained under a pressure of 9 MPa for 15 s, ensuring its good encapsulation.

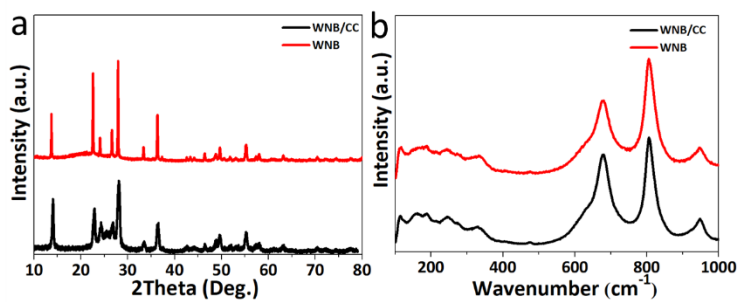


Fig. S1 The images of XRD and Raman for WNB and WNB/CC.

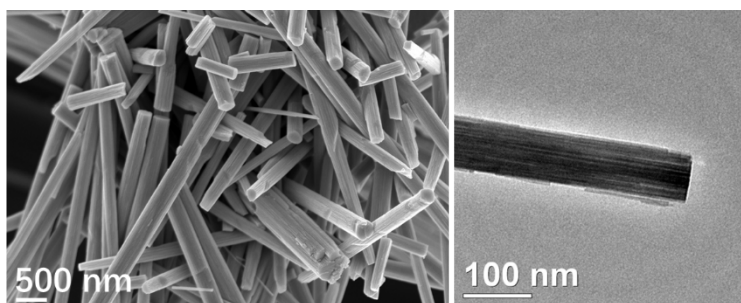


Fig. S2 FESEM and TEM images of WNB.

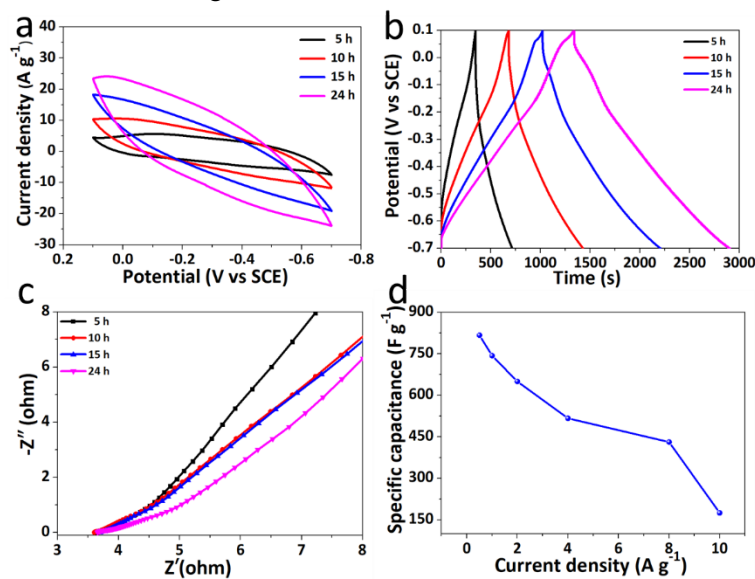


Fig. S3 (a-c) Comparison of CV, GCD, and EIS curves for the as-synthesized WO_3 sample with different time at the same test condition. (d) Specific capacitance of the WNB/CC products at different current densities.

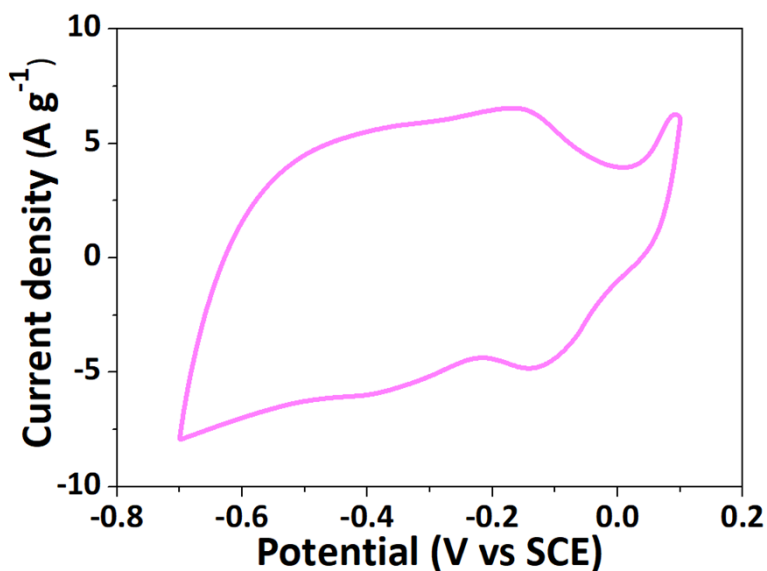


Fig. S4 CV curve of WNB/CC electrodes at 2mV s^{-1} .

Fig. S5 CV curves of CC, WNB and WNB/CC electrodes at 20mV s^{-1} .

Fig. S6 Cycling performance of WNB/CC electrode.

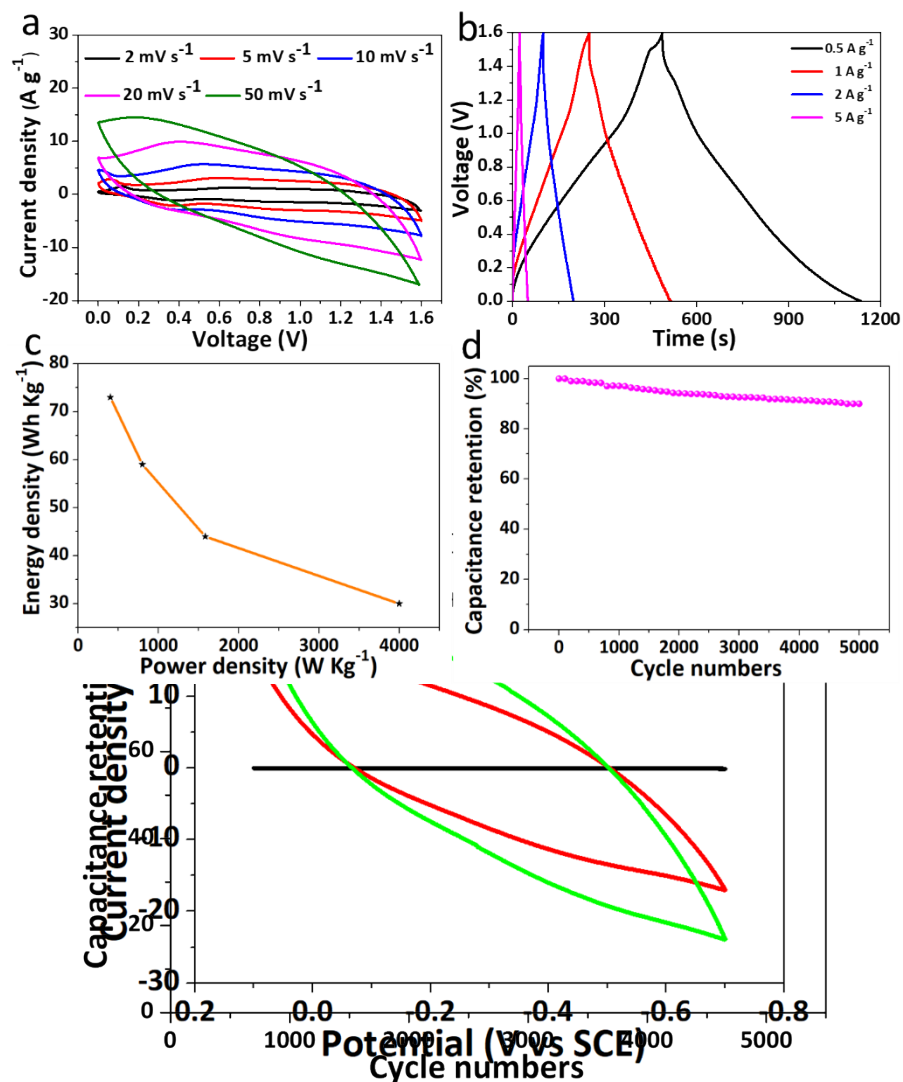


Fig. S7 (a) CV curves of symmetric supercapacitors device at different scan rates. (b) GCD curves of the symmetric supercapacitors device at different current densities. (c) Ragone plot of the symmetric supercapacitors device. (d) Cycling performance of the symmetric supercapacitors device.